

Article

Wheat Leaf Rust Fungus Effector Protein Pt1641 Is Avirulent to TcLr1

Jiaying Chang ¹, Johannes Mapuranga ¹, Ruolin Li ¹, Yingdan Zhang ¹, Jie Shi ², Hongfei Yan ^{1,*} and Wenxiang Yang ^{1,*}

¹ Technological Innovation Center for Biological Control of Plant Diseases and Insect Pests of Hebei Province, College of Plant Protection, Hebei Agricultural University, Baoding 071000, China; changjiaying@163.com (J.C.); jmapuranga@hotmail.com (J.M.); m15369870831@163.com (R.L.); 15733719705@163.com (Y.Z.)

² International Science and Technology Joint Research Center on IPM of Hebei Province, IPM Innovation Center of Hebei Province, Key Laboratory of Integrated Pest Management on Crops in Northern Region of North China, Ministry of Agriculture and Rural Affairs, Plant Protection Institute, Hebei Academy of Agriculture and Forestry Sciences, Baoding 071000, China; shij99@163.com

* Correspondence: hongfeiyang2006@163.com (H.Y.); wenxiangyang2003@163.com (W.Y.)

Abstract: Wheat leaf rust fungus is an obligate parasitic fungus that can absorb nutrients from its host plant through haustoria and secrete effector proteins into host cells. The effector proteins are crucial factors for pathogenesis as well as targets for host disease resistance protein recognition. Exploring the role of effector proteins in the pathogenic process of *Puccinia triticina* Eriks. (*Pt*) is of great significance for unraveling its pathogenic mechanisms. We previously found that a cysteine-rich effector protein, Pt1641, is highly expressed during the interaction between wheat and *Pt*, but its specific role in pathogenesis remains unclear. Therefore, this study employed techniques such as heterologous expression, qRT-PCR analysis, and host-induced gene silencing (HIGS) to investigate the role of Pt1641 in the pathogenic process of *Pt*. The results indicate that Pt1641 is an effector protein with a secretory function and can inhibit BAX-induced programmed cell death in *Nicotiana benthamiana*. qRT-PCR analyses showed that expression levels of *Pt1641* were different during the interaction between the high-virulence strain THTT and low-virulence strains FGD and Thatcher, respectively. The highest expression level in the low-virulence strain FGD was four times that of the high-virulence strain THTT. The overexpression of *Pt1641* in wheat near-isogenic line TcLr1 induced callose deposition and H₂O₂ production on TcLr1. After silencing *Pt1641* in the *Pt* low-virulence strain FGD on wheat near-isogenic line TcLr1, the pathogenic phenotype of *Pt* physiological race FGD on TcLr1 changed from “,” to “3”, indicating that Pt1641 plays a non-toxic function in the pathogenicity of FGD to TcLr1. This study helps to reveal the pathogenic mechanism of wheat leaf rust and provides important guidance for the mining and application of *Pt* avirulent genes.

Keywords: *Puccinia triticina*; effector protein; avirulence function; TcLr1; resistance



Citation: Chang, J.; Mapuranga, J.; Li, R.; Zhang, Y.; Shi, J.; Yan, H.; Yang, W. Wheat Leaf Rust Fungus Effector Protein Pt1641 Is Avirulent to TcLr1. *Plants* **2024**, *13*, 2255. <https://doi.org/10.3390/plants13162255>

Academic Editor: Haiguang Wang

Received: 29 June 2024

Revised: 12 August 2024

Accepted: 13 August 2024

Published: 14 August 2024



Copyright: © 2024 by the authors. Licensee MDPI, Basel, Switzerland. This article is an open access article distributed under the terms and conditions of the Creative Commons Attribution (CC BY) license (<https://creativecommons.org/licenses/by/4.0/>).

1. Introduction

Plants are attacked by various pathogens during their growth. In the process of interaction between plants and pathogens, on one hand, the pathogens plunder nutrients from the host plant cells to maintain survival and reproduction, while on the other hand, the host plants use various defense mechanisms to inhibit the invasion, growth, and reproduction of pathogens. Pathogens secrete a variety of effector proteins targeting different sites in host plant cells during infection to disrupt a series of defense reactions in plant cells [1,2]. Effector proteins are important pathogen virulence factors, but they are also targets of host disease resistance proteins, making them a double-edged sword [3]. Effector proteins that can be specifically recognized by plant disease resistance (*R*) genes are known as avirulence (*Avr*) genes, while those not recognized are referred to as virulence genes.

Plant disease resistance proteins can recognize effectors through two types of mechanisms, with the most common one being direct recognition, often known as the “receptor-ligand model” [4,5], such as the recognition patterns of wheat stem rust resistance genes *Sr35*, *Sr50*, and *Sr27* with the corresponding *AvrSr35*, *AvrSr50*, and *AvrSr27* of stem rust fungus [6–8]. Flax’s L5/L6 proteins directly recognize the pathogen’s effector protein *AvrL567* and trigger downstream immune responses [9]. After being transported into plant cells, the rice blast fungus avirulent protein *Avr-Pita* can directly bind to the LRD region of the N-terminal of the plant *Pita* protein, triggering downstream signaling pathways to induce disease resistance responses [10,11]. The other type of recognition mechanism is indirect recognition, which comprises two ways. One involves host surveillance proteins recognizing effector proteins and activating disease resistance proteins to trigger immune responses, and it is often referred to as the “guard model”, for example, the recognition mechanisms between *RIN4*, *RPM1*, and *RPS2* in *Arabidopsis thaliana* with *AvrRpm1*, *AvrB*, and *AvrRpt2* [12]. The second one involves the effectors targeting decoy proteins and modifying them to elicit disease resistance protein recognition towards the effector proteins, and it is often referred to as the “decoy model” [13,14], for instance, the recognition of *RRS1/RPS4* with *PopP2* in *Arabidopsis thaliana* [15] and the recognition of soybean Glucanase Inhibitor Protein (*GmGIP1*) with the pathogen-secreted *PsXEG1-Like Protein* (*PsXLP1*) in *Phytophthora soya* [16,17]. These examples clearly illustrate that the recognition mechanisms of disease resistance proteins towards effectors are highly complex. Therefore, gaining a deeper understanding of the interactions between pathogen effector proteins and host disease resistance proteins is crucial for unraveling pathogen pathogenicity and immune induction mechanisms.

Wheat leaf rust is a biotrophic fungus, and the haustorium is its important nutritional organ and the site for secreting effectors [18,19]. However, there are currently few reports about *Pt* avirulent genes. *Pt3* and *Pt27* were identified as candidate avirulent genes corresponding to *Lr9*, *Lr24*, and *Lr26* in wheat [20]. Six hundred thirty-five *Pt* candidate effector proteins were screened through a transcriptome analysis, among which the candidate effector proteins *Pt77192*, *Pt5974*, *Pt34354*, *Pt23713*, *Pt1625*, and *Pt36553* were upregulated during the interaction between *Pt* and wheat, and these may potentially play diverse roles in the pathogenic process of *Pt* [21]. The integration of the genomic and association analysis approach identified 20 candidate effector proteins for *Lr20* [22]. A study based on long-read de novo assembly and comparative genomics also discovered candidate effector proteins for *Lr26*, *Lr2a*, and *Lr3ka* [23]. Recently, transcriptome analysis of a *Pt* mutant strain with virulence against *Lr19* identified eight secreted proteins as *AvrLr19* candidate proteins [24]. Furthermore, another transcriptome study integrated with computational analysis identified six candidate effector proteins for the leaf rust resistance gene *Lr28*, among which *Lr28* was found to strongly bind to the candidate protein *c14094_g1_i1*, forming a stable complex [25]. Nevertheless, only a few *Pt* effector proteins have been successfully cloned and functionally characterized, such as *Pt13024* [26] and *Pt_21* [27]. At present, the research on the function of wheat leaf rust fungus effector proteins is still in its early stages. The role of effector proteins secreted by pathogens in pathogenicity still needs to be further studied, and clarification on the function of effector proteins is of great significance for unravelling new methods of disease resistance.

In this study, we screened candidate effector proteins that were highly expressed during the interaction between wheat and *Pt* and obtained a cysteine-rich effector protein, *Pt1641*, with a secretory function. The effector protein was highly expressed during the initial stages of infection, and its expression trend and level were different in different pathogenic physiological races. *Pt1641* targets the cell membrane, inhibits BAX-induced cell death, and triggers H_2O_2 accumulation and callose deposition on the wheat near isogenic line *TcLr1*. Silencing *Pt1641* from the low-virulence race *FGD* in *TcLr1* enhanced the pathogenicity of *Pt* (*FGD*) on *TcLr1*, and the infection type changed from “;” to “3”, indicating that *Pt1641* is avirulent to *TcLr1*.

2. Results

2.1. *Pt1641* Is an Effector Protein Secreted by *Pt*

A highly expressed candidate effector protein, *Pt1641*, was selected from the transcriptome database of *Pt* inoculated on the wheat near-isogenic line Thatcher (Tc). *Pt1641* consists of 141 amino acids, including 11 cysteines, accounting for 7.8% of the total, and has a predicted molecular weight of 15.72 kDa. Signal peptide prediction using the SignalP-5.0 online software tool revealed that *Pt1641* contains a signal peptide located at amino acids 1–20. ApoplastP predicted that it is localized in the apoplast. Using the TMHMM transmembrane domain prediction online software, we found that the effector protein *Pt1641* lacks a transmembrane domain and does not contain any known protein domains. We used the TTC reduction method to detect the enzymatic activity of secreted invertase to verify whether the signal peptide of candidate effector protein *Pt1641* has a secretory function. The results showed that the signal peptides of *Pt1641* and *Avr1b* (positive control) can secrete the invertase to hydrolyze sucrose in the solution into monosaccharides. The TTC reaction with monosaccharides formed a red insoluble compound, triphenylmethane (red precipitate), while *Mg87* and the empty strain (negative control) could not form a red precipitate, demonstrating that the *Pt1641* signal peptide has a secretory function (Figure 1).

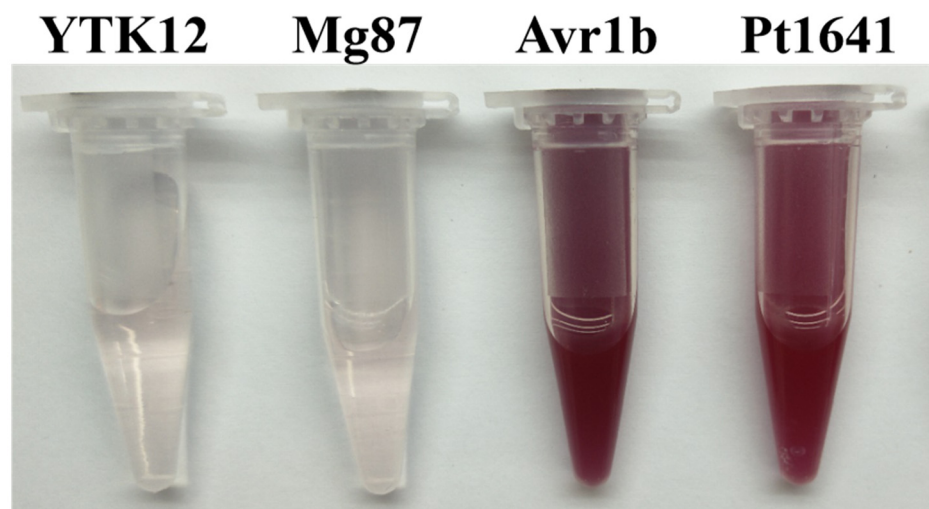


Figure 1. A photograph of microtubes showing the functional validation of the *Pt1641* signal peptide using the yeast invertase secretion assay. Yeast strain YTK12 carrying pSUC2-*Avr1b* served as a positive control, and YTK12 and YTK12 carrying pSUC2-*Mg87* were used as a negative control. Secreted invertase can catalyze the reduction of 2,3,5-triphenyltetrazolium chloride (TTC) to form insoluble red 1,3,5-triphenyl formazan (TPF). The presence of a red color confirms the occurrence of invertase activity.

2.2. Transcriptional Expression Characteristics of *Pt1641*

The transcript levels of *Pt1641* were detected by qRT-PCR during the interaction between Tc and two *Pt* physiological races with different virulence. During the interaction between the high-virulence strain THTT and Tc, compared with urediospores, the *Pt1641* expression level was upregulated from 6 h post-inoculation (hpi) and reached its peak at 36 hpi, which is a critical stage for haustoria formation and the suppression of the plant's initial defense response (Figure 2A). During the interaction between the low-virulence strain FGD and Tc, the expression level of *Pt1641* started to increase at 6 hpi and peaked at 24 hpi, approximately 20 times higher than at the urediospores, a crucial period for the formation of the haustorial mother cells (Figure 2B). At different infection stages, *Pt1641* exhibited higher expression levels in the low-virulence race FGD compared to the high-virulence race THTT, indicating variations in expression levels among different races.

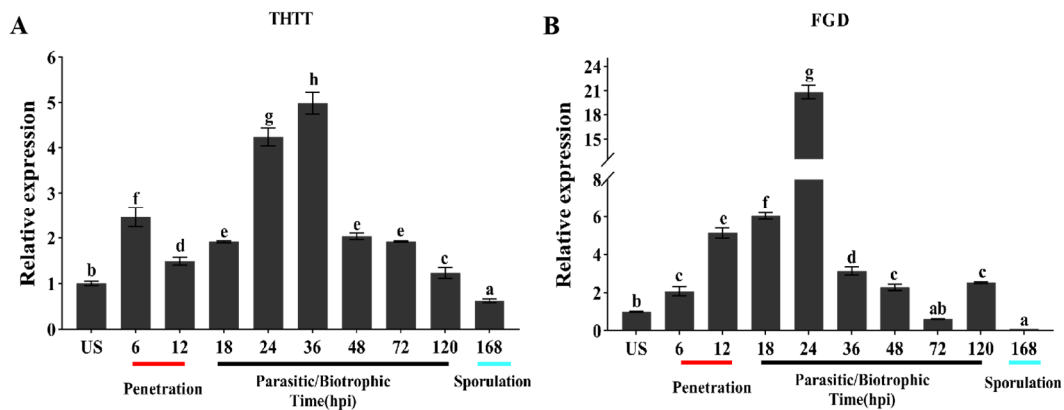


Figure 2. Transcription profiles of *Pt1641* in different *Pt* physiological races. The expression level of *Pt1641* was assayed with RNA isolated from urediniospores (US), and leaves of wheat cultivar Thatcher were inoculated with *Pt* sampled at 6, 12, 18, 24, 36, 48, 72, 120, and 168 hpi. The relative expression was calculated by the comparative $2^{-\Delta\Delta C_t}$ method. The standard deviation and the mean fold changes were calculated with the results from three independent biological replicates. The letters indicate the significant difference compared to urediniospores ($p < 0.05$, unpaired two-tailed Student's *t*-test). (A) Expression patterns of *Pt1641* on Thatcher inoculated with THTT. (B) Expression patterns of *Pt1641* on Thatcher inoculated with FGD.

2.3. *Pt1641* Has a Toxic Function

To determine whether *Pt1641* possesses potential toxic functions, we tested *Pt1641* for its inhibitory effects on BAX-induced PCD in *Nicotiana benthamiana* cells. Both *Pt1641* and *Avr1b* (positive control) inhibited BAX-induced PCD, while the negative control, GFP, could not suppress cell death (Figure 3A). The decolorization of *N. benthamiana* with alcohol resulted in a clear observation of cell death (Figure 3A). WB detection proved that the protein was successfully expressed (Figure 3B). These results showed that the transient expression of effector protein *Pt1641* suppressed Bax-induced cell death, indicating that it has toxic functions.

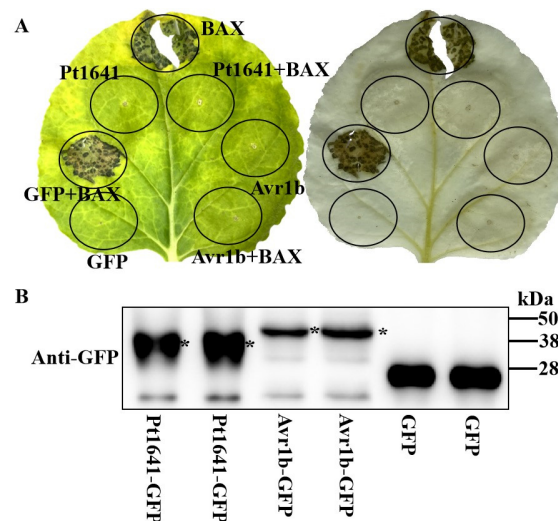


Figure 3. *Pt1641* inhibits BAX-induced plant cell PCD. (A) *Pt1641* was transiently expressed in *Nicotiana benthamiana*, and BAX was injected 24 h later. The same leaf was examined before (right) and after (left) staining with a decolorizing solution. (B) Protein expression was detected by Western blotting. *Agrobacterium tumefaciens* containing *Pt1641*-GFP, *Avr1b*-GFP, and GFP was injected into tobacco leaves, and BAX was injected 24 h later. After 48 h, proteins were extracted from tobacco leaves and incubated with primary anti-GFP to detect protein expression. * Target protein.

2.4. Pt1641 Acts on the Cell Membrane

Identifying the action site of effector protein Pt1641 in plant cells is of great significance for studying its role during the interaction between wheat and *Pt*. Pt1641-GFP, Pt1641^{ΔSP}-GFP, and GFP were expressed in *N. benthamiana* cells using a transient expression technique mediated by *Agrobacterium tumefaciens*. The green fluorescence signal was observed in the whole cells of tobacco expressing GFP, and the GFP fluorescence signal was observed in the cell membrane of *N. benthamiana* expressing Pt1641-GFP. In *N. benthamiana* cells expressing Pt1641^{ΔSP}-GFP, significant GFP fluorescence signals were observed in the whole cells. These results indicate that the effector protein Pt1641 acts on the cell membrane (Figure 4A). WB detection proved that the protein was successfully expressed (Figure 4B).

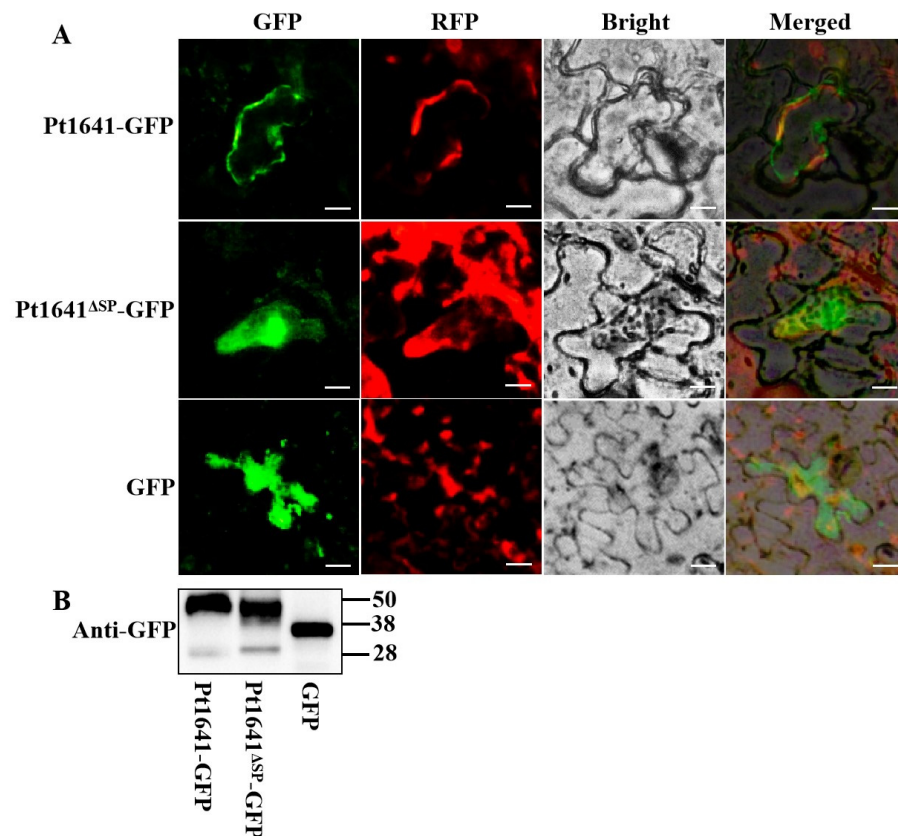


Figure 4. Pt1641 accumulates in the cytomembrane of *N. benthamiana*. (A) Leaf tissues of *N. benthamiana* transiently co-expressing Pt1641-GFP, Pt1641^{ΔSP}-GFP, and GFP were examined by epifluorescence microscopy. Bars = 50 μ m. (B) Protein expression was detected by Western blotting. *Agrobacterium tumefaciens* containing Pt1641-GFP, Pt1641^{ΔSP}-GFP, and GFP was injected into tobacco leaves. After 48 h, proteins were extracted from tobacco leaves and incubated with primary anti-GFP to detect protein expression.

2.5. Pt1641 Stimulates Callose Deposition and H₂O₂ Production on TcLr1

Using the bacterial type III secretion system (T3SS), we overexpressed Pt1641 in 40 near-isogenic lines (Supplementary Figure S1) and found that it promoted callose deposition and the accumulation of H₂O₂ on wheat near-isogenic line TcLr1. Therefore, we selected TcLr1 as the research object. After transiently expressing the effector protein Pt1641 in TcLr1, the effect of Pt1641 on callose deposition and H₂O₂ accumulation was observed. The results showed that compared with the leaves injected with EtHAN-pEDV6 and MgCl₂ buffer, we could clearly observe callose deposition and H₂O₂ accumulation in leaves injected with EtHAN-Pt1641, indicating that Pt1641 can induce callose deposition (Figure 5A) and H₂O₂ accumulation (Figure 5B) in TcLr1.

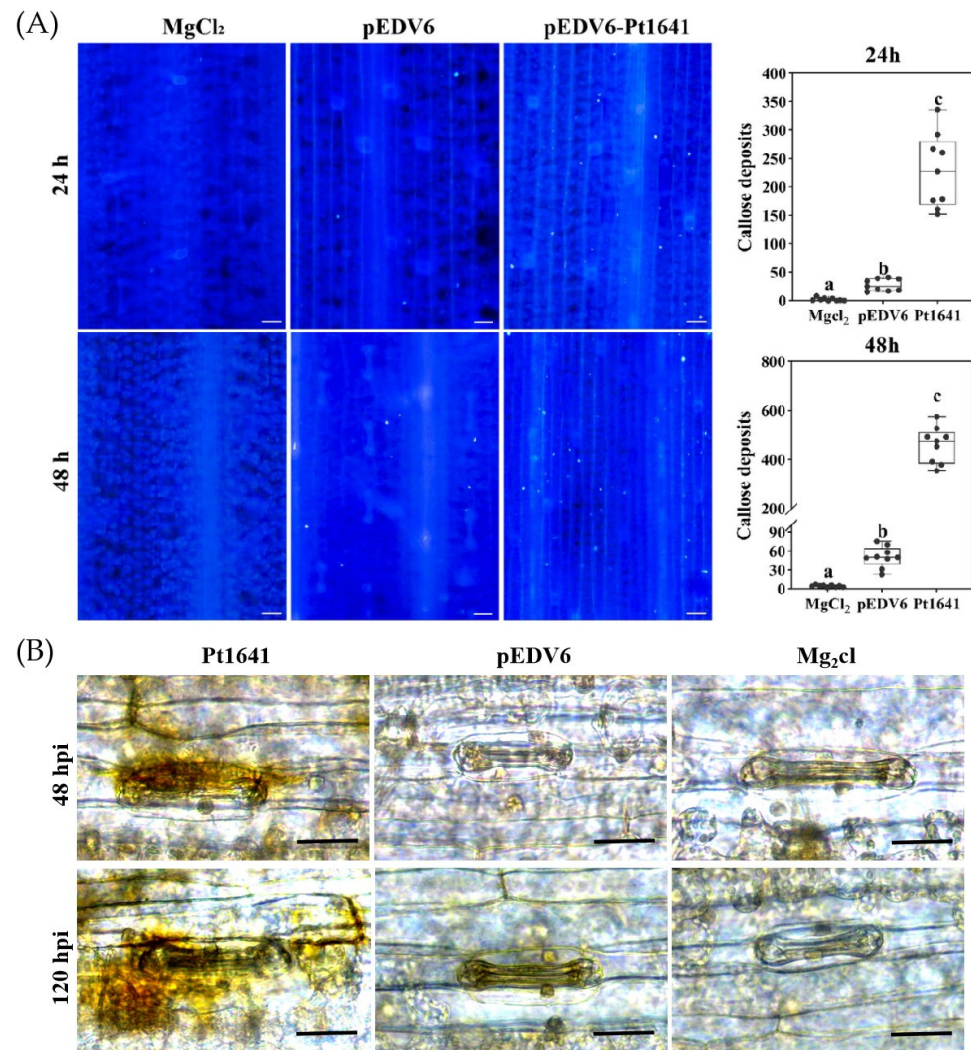


Figure 5. Pt1641 induces callose deposition and the accumulation of H₂O₂ on TcLr1. **(A)** Wheat leaf samples were collected at 24 and 48 h after the infiltration of TcLr1 with EtHAN. After decolorization, the leaves were stained overnight with 0.05% aniline blue. MgCl₂ and pEDV6 served as blank controls. Images were captured under a fluorescence microscope. Bar = 200 μ m. The mean values and standard deviations were obtained from nine 1 mm² areas of 3 biological replicates. Letters represent significant differences ($p < 0.05$). **(B)** Wheat leaf samples were collected at 48 and 120 h after the infiltration of TcLr1 with EtHAN. After DAB (1 mg/mL) staining, the accumulation of H₂O₂ was observed, and the images were captured under a light microscope. MgCl₂ and pEDV6 served as blank controls. Bar = 20 μ m.

2.6. Pt1641 Has Non-Toxic Function on TcLr1

To clarify the function of the effector protein Pt1641 during the infection of the low-virulence physiological race FGD on TcLr1, we employed barley stripe mosaic virus (BSMV)-mediated host-induced gene silencing (HIGS) technology to silence its transcription levels. Plants inoculated with BSMV:*TaPDS* in TcLr1 exhibited bleaching, while mild yellowing and mosaic symptoms were observed on TcLr1 leaves inoculated with BSMV:*Pt1641* and BSMV:00, indicating the effective work of the virus system. The BSMV-inoculated leaves of wheat plants were further challenged with a low-virulence *Pt* race FGD. The disease phenotypes were observed fourteen days post inoculation. Compared with control plants, in TcLr1 plants with silenced *Pt1641*, the pathogenic phenotype of *Pt* physiological race FGD changed from “;” to “3”, and obvious uredinium piles appeared, indicating that Pt1641 plays a non-toxic function in the pathogenicity of FGD to TcLr1 (Figure 6A). qRT-

PCR analyses showed that the *Pt1641* expression level was reduced by 59.03–66.79% at 24 and 48 hpi, respectively, in TcLr1 plants inoculated with BSMV:*Pt1641* (Figure 6B) compared to the control plants inoculated with BSMV:00, indicating that *Pt1641* was successfully silenced.

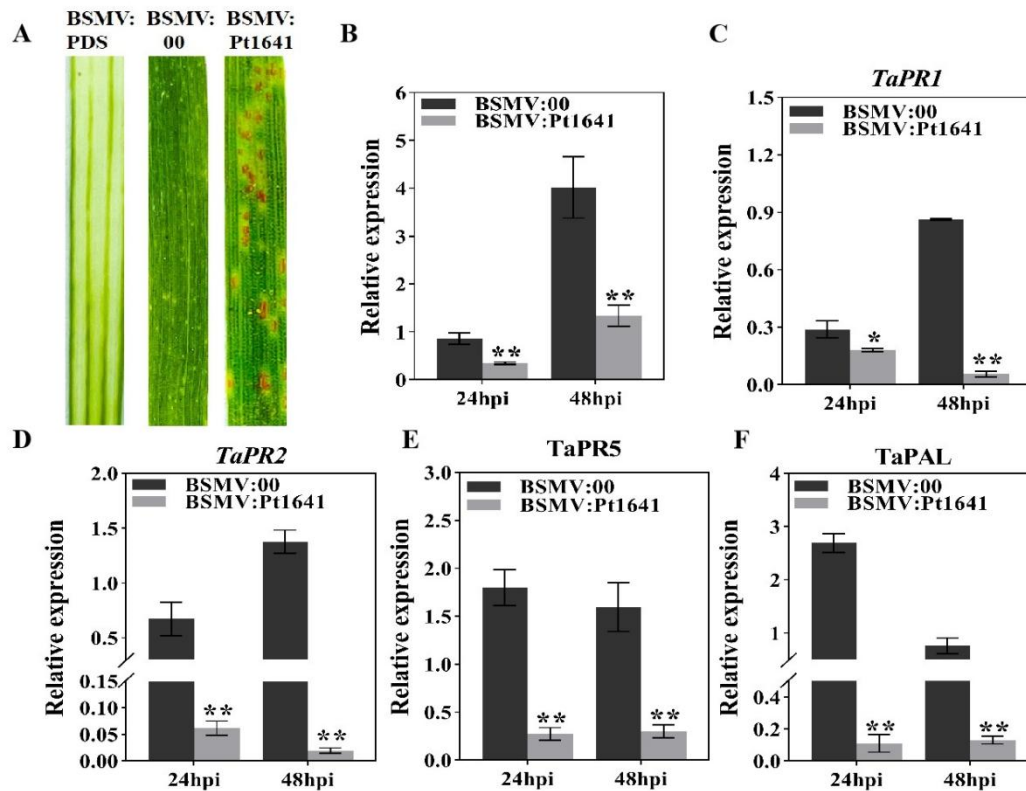


Figure 6. The BSMV-mediated silencing of *Pt1641* in wheat. (A) A photograph of phenotypes of wheat leaves of TcLr1 14 days post *Puccinia triticina* inoculation after silencing *Pt1641*. (B) The silencing efficiency in *Pt1641* knockdown wheat leaves was assessed using qRT-PCR. The samples were collected for RNA extraction from the 3 leaves of wheat plants at 24 and 48 hpi. The mean and standard deviation were calculated from three independent biological replicates. (C–F) The expression levels of different genes were assessed in TcLr1. The asterisks indicate a significant difference in samples with *Pt1641*-silenced plants in comparison with the control (* $p < 0.05$; ** $p < 0.01$).

To clarify the impact of *Pt1641* on wheat resistance during the infection process of the *Pt* low-virulence physiological race FGD, we analyzed the expression levels of different disease resistance-related genes using qRT-PCR. The results showed that the expression levels of disease resistance-related genes *TaPR1*, *TaPR2*, and *TaPR5* and salicylic acid synthesis pathway-related gene *TaPAL* significantly decreased in *Pt1641*-silenced plants compared to the control plants (Figure 6C–F), suggesting that *Pt1641* can inhibit TcLr1 immune response.

3. Discussion

Plants growing in nature face various biological stresses from the surrounding environment. To enhance their survival, plants evolved a more intricate defense system to perceive and defend themselves against plant pathogens [28,29]. However, pathogens can affect the signal transduction and normal function of the host cell by secreting effector proteins that manipulate the host immune responses [1]. Specific disease resistance proteins (R proteins) in plants can directly or indirectly recognize effector proteins secreted by pathogens and trigger plant resistance responses [28]. However, in the long-term co-evolution, new R proteins and effector proteins continue to emerge, thus forming a complex interaction network between plants and pathogens, whereby pathogens endure

evolutionary changes to evade host immunity, while hosts are subject to selective pressures that favor the elimination of pathogens [29,30]. Identifying pathogen effector proteins that stimulate *R* gene-mediated disease resistance is of significant practical value in developing disease-resistant plant varieties.

Wheat leaf rust resistance protein *Lr1* is a race-specific leaf rust resistance protein and a typical *R* protein. Since the successful cloning of *Lr1* in 2007, there have been no reports of any effector protein that stimulates the expression of *Lr1* protein resistance [31]. Effector proteins are a class of proteins that are synthesized in pathogen cells and then secreted into the extracellular space, then act on the surface of the plant plasma membrane, act in the plasma membrane space, or enter into host cells to exert their effects [1,32]. Therefore, effector proteins are important targets for the recognition of disease resistance proteins in host plants. However, there are few studies on the functional characterization of avirulent genes of wheat leaf rust; for example, PTTG_08198 accelerated the process of cell death and promoted the accumulation of reactive oxygen species (ROS) [33]. Pt13024 was found to inhibit programmed cell death (PCD), trigger ROS accumulation and callose deposition, and exhibit a non-toxic function on TcLr30 [26]. Pt_21 inhibited host defense responses by directly targeting wheat TaTLP1 and suppressing its antifungal activity [27]. Avirulent protein AvrLr15 from *Pt* can induce *Lr15*-dependent immune responses [34]. Hence, the study of the effector protein that stimulates *Lr1* resistance is of great significance for the effective control of *Pt* and the development of durable leaf rust-resistant cultivars. In this study, the candidate effector protein Pt1641 was obtained by screening the transcriptome database of wheat infected by *Pt*. A bioinformatics analysis and yeast invertase secretory assay demonstrated that Pt1641 is a secreted protein of *Pt*, which consists of 141 amino acids with 11 cysteine residues and a signal peptide at the N-terminal from the 1–20 aa.

Pt1641 was overexpressed in 40 near-isogenic lines (Supplementary Figure S1), and its performance varied in different near-isogenic lines. In some near-isogenic lines, it can inhibit the accumulation of callose and H₂O₂, while in other near-isogenic lines, it can promote the accumulation of callose and H₂O₂ but to varying extents. It significantly promoted callose deposition and H₂O₂ accumulation in TcLr1. This implies that Pt1641 was highly recognized by TcLr1 compared to other near isogenic lines. No relevant studies have been reported on TcLr1. In this study, after silencing *Pt1641* in FGD, a *Pt* low-virulence physiological race, its virulence to TcLr1 was significantly enhanced, indicating that Pt1641 plays a non-toxic role in the infection of TcLr1 by FGD. The *Pt1641* expression level and trend in different physiological races were different, and the expression level was relatively high during the interaction between FGD and Tc. Therefore, Pt1641 is easily recognized by *Lr1*, which may also be the reason why FGD exhibits low virulence on TcLr1. The expression levels of genes in different virulent physiological species have not been studied, so this study provides a new idea for the study of avirulent genes. Currently, most of the studies on avirulent genes have only analyzed their polymorphisms in different physiological species [26,35–37], but no specific research has studied the expression of these genes in different physiological races.

Magnaporthe oryzae resistance gene *Pita* encodes a cytoplasmic membrane receptor protein of 928 amino acids, including NBS and leucine-rich domains, in which amino acid 918 is critical in controlling resistance (resistance is lost when alanine is changed to serine) [10]. The *M. oryzae* effector protein AVR-*Pita* directly interacts with *Pita* in a typical mode [10]. On the other hand, *Lr1*, which belongs to a larger *psr567* gene family, has CC-NBS-LRR domains. A transmembrane domain was predicted at the N-terminal of the *Lr1* protein, suggesting that its location may be close to the cell membrane, perhaps as part of a membrane-binding complex [31]. A subcellular localization analysis in *N. benthamiana* revealed that Pt1641 acts on the cell membrane, same as the predicted location of *Lr1*. An AlphaFold 3 prediction analysis demonstrated a potential interaction between Pt1641 and *Lr1*, suggesting a high probability of direct interaction [38,39]. Our subsequent experiments aim to unravel and clarify the molecular mechanisms underlying the interaction between Pt1641 and *Lr1*. Intramolecular disulfide bonds formed by cysteine are thought to play an

important role in enhancing the stability of effector proteins in host cells [40]. The effector protein Pt1641 contains 11 cysteine residues, with one cysteine present in the signal peptide. Therefore, in our subsequent research, we aim to further analyze the amino acid sequence polymorphism of Pt1641 in different virulent physiological races as well as the content of its cysteine residues. This analysis will help to elucidate whether the sequence variation in Pt1641 is related to the different defense responses of TcLr1 to different *Pt* virulent races.

This study revealed that the *Pt* effector protein Pt1641 is a secreted protein that functions on the cell membrane, and it can inhibit BAX-induced PCD in *N. benthamiana*. Pt1641 exhibits varying expression levels and trends among different *Pt* physiological races, with relatively higher expression levels during the interaction between FGD and Tc. In wheat near-isogenic line TcLr1, Pt1641 can induce callose deposition and H₂O₂ accumulation, indicating that it has the ability to stimulate TcLr1 resistance. Silencing *Pt1641* in FGD on TcLr1 by HIGS resulted in a change in the pathogenic phenotype of FGD from “;” to “3”, indicating enhanced pathogenicity. This suggests that Pt1641 plays a non-toxic role on TcLr1, that is, Pt1641 is avirulent to TcLr1. This study provides a molecular basis for exploring avirulent genes in *Pt*, which can be used to identify corresponding wheat disease resistance genes that can be utilized as tools to carry out genetic engineering research and promote the development of new varieties, which has important practical value for *Pt* disease resistance breeding.

4. Materials and Methods

4.1. Sequence Analysis

The Pt1641 sequence was derived from the transcriptome database of wheat infected with *Pt*. Signal peptide identification of Pt1641 was performed using SignalP 5.0 (<https://services.healthtech.dtu.dk/services/SignalP-5.0/> (accessed on 1 June 2024)). The localization of the secreted protein was predicted by Apoplast P 1.0 (<https://apoplastp.csiro.au/index.html> (accessed on 1 June 2024)). TMHMM 2.0 (<https://services.healthtech.dtu.dk/services/TMHMM-2.0/> (accessed on 1 June 2024)) was utilized to predict the presence of a transmembrane domain within the effector protein Pt1641. The interaction between Pt1641 and Lr1 was predicted by AlphaFold 3 analysis [38,39]. All primers used in this study are described in Supplementary Data S1.

4.2. Expression Analysis of *Pt1641*

Using Thatcher and Thatcher-Lr1 as the research objects, we inoculated Thatcher with the *Pt* high-virulence strain THTT and the low-virulence strain FGD, and they were maintained at 25 °C. The response of various leaf rust resistance genes to these *Pt* races was explained by Long and Kolmer (1989) [41] in their proposed nomenclature system that designated the virulence of cultures of *Pt* combinations. We collected infected leaves of Thatcher at 0, 6, 12, 18, 24, 36, 48, 72, 120, and 168 h post-inoculation (hpi). Total RNA was extracted from the infected wheat leaves using total RNA purification kit (Sangon Biotech (Shanghai, China)). Subsequently, cDNA was synthesized through reverse transcription using EasyScript One-Step gDNA Removal and cDNA Synthesis SuperMix (Transgen, Beijing, China AE311). qRT-PCR was performed on QuantStudio 5 (ThermoFisher, Waltham, MA, USA). The expression level of *Pt1641* was analyzed with *PtActin* as the reference gene. The relative expression of *Pt1641* was calculated by $2^{-\Delta\Delta C_t}$ method. Standard deviations and averages were calculated from results of three independent biological replicates. Statistical significance was assessed using a Student's *t*-test.

4.3. Validation of the Secretory Function of *Pt1641* Signal Peptide

To validate the secretory function of the predicted signal peptide of Pt1641, we used the yeast signal sequence trap system [42]. The predicted Pt1641 signal peptide sequence was cloned into the vector pSUC2T7M13ORI (pSUC2) using specific primers, then transformed into the invertase-deficient yeast strain YTK12 and incubated at 30 °C [43]. The positive colonies were screened with CMD-W medium, and then, the invertase enzyme activity

was detected through its ability to reduce 2,3, 5-triphenyltetrazolium chloride (TTC) to insoluble red 1,3,5-triphenylformic acid (TPF) [44].

4.4. Pt1641 Transient Expression in *Nicotiana benthamiana*

In order to detect whether Pt1641 can inhibit the PCD induced by Bax, PVX-Pt1641 (without signal peptide) was cloned into pGR106 to construct PVX-Pt1641-GFP plasmid, which was transformed into *Agrobacterium tumefaciens* GV3101. It was then cultured in Luria–Bertani medium containing 25 mg L⁻¹ rifampicin and 50 mg L⁻¹ kanamycin. GV3101 carrying the corresponding construct was suspended in acetylsyringone buffer (10 mM MgCl₂, 10 μM AS, 10 mM 2-(N-morpholino) methanesulfonic acid (MES), pH 5.6), and strains containing GFP, Avr1b-GFP, and Pt1641^{ΔSP}-GFP with an OD₆₀₀ of 0.5 were injected into 4-week-old tobacco leaves. Twenty-four hours later, the GV3101 strain containing the BAX gene was injected at the same location. Leaf necrosis was observed at 7 days post-infiltration (dpi), and the *N. benthamiana* leaves were decolorized in ethanol/acetic acid (1:1) until semi-translucent, followed by photographing them. To observe the sub-cellular localization of Pt1641 in tobacco cells, strains containing GFP, Pt1641-GFP, and Pt1641^{ΔSP}-GFP were mixed with RFP-labeled GV3101 bacterial solution in a 1:1 ratio and injected into tobacco leaves. After 48 h, TI2-U inverted fluorescence microscope (Nikon, Minato City, Japan) was used to observe and photograph them.

4.5. Bacterial T3SS-Mediated Pt1641 Overexpression in Wheat

The constructs pEDV6 and pEDV6-Pt1641 were electroporated into the *Pseudomonas fluorescens* EtHAN. The bacteria were cultured in King's medium containing antibiotics (50 mg/L spectinomycin and 30 mg/L chloramphenicol) for 48 h. After the bacteria were collected, they were washed twice with 10 mM MgCl₂, and *Pseudomonas fluorescens* (OD₆₀₀ was 1.0) were infiltrated into the second wheat leaves. Samples were collected at 24 and 48 hpi to detect callose deposition. The leaves were decolorized with acetic acid/ethanol (1:1) for 24 h, then washed twice with 50% ethanol for 15 min each time with a 10 min water rinse, washed with 0.5 M NaOH for 10 min with a 10 min water rinse, and finally washed with 67 mM K₂HPO₄ (pH 9.0) for 1 h. Leaf samples were stained overnight with 0.05% aniline blue in 67 mM K₂HPO₄ (pH 9.0) [45]. The leaves were rinsed with water, soaked in 50% glycerol, and examined with DAPI filter under TI2-U inverted fluorescence microscope (Nikon). The amount of callose deposition was quantified using ImageJ-win64 software [46]. For the detection of H₂O₂ accumulation, the inoculated leaves were sampled at 48 and 120 hpi, and 3, 30-diaminobenzidine (DAB) staining was used to determine the accumulation of H₂O₂, which was then observed under a microscope.

4.6. BSMV-Mediated Gene Silencing

To investigate the role of Pt1641 during the infection of TcLr1 with low-virulence strain FGD, the Pt1641 was silenced on TcLr1 by HIGS technique. Specific fragments were cloned and inserted into barley stripe mosaic virus (BSMV) to generate BSMV:γ:Pt1641, which was then transformed into EHA105. Following the protocol used by Qi et al. [44], the BSMV virus was propagated on tobacco leaves. Tobacco leaves containing BSMV were ground in PBS buffer and diatomaceous earth and applied with gloved fingers to the second leaf of two-leaf wheat [47]. BSMV:TaPDS encoding a plant phytoene desaturase was used as positive control, and wheat seedlings inoculated with only BSMV:γ were used as negative control. Fourteen days after virus inoculation, the fourth wheat leaves were inoculated with fresh FGD strain and maintained under humid conditions at 25 ± 3 °C. The Pt pathogenic phenotype was observed at 14 dpi (infection type: “0” no uredinium or infection court; “;” no uredinium, but there is necrosis or chlorosis; “1” the uredinium are small and have necrotic spots around them; “2” uredinium are small to medium, with necrosis or chlorosis around them; “3” the uredinium is medium, with or without chlorosis; “4” uredinium is large, without chlorosis and necrosis, often satellite uredinium). The leaves inoculated with FGD were collected at 0, 24, and 48 hpi, respectively, for RNA isolation

and histological observation. RNA extraction from three leaf samples was performed to evaluate the silencing efficiency. The transcriptional expression of *TaPR1*, *TaPR2*, *TaPR5*, and *TaPAL* was detected using *TaEF* as internal parameter.

Supplementary Materials: The following supporting information can be downloaded at <https://www.mdpi.com/article/10.3390/plants13162255/s1>, Figure S1: The effect of P1641 on callose in different near-isogenic lines. The amount of callose on near-isogenic lines was analyzed for significant differences using unpaired two-tailed Student's *t* test. The asterisk (*) denotes a significant difference in callose deposition between pEDV6 and Pt1641 on the same near-isogenic line ($p < 0.05$). Data S1: Primers used in this study.

Author Contributions: W.Y., J.C. and H.Y. designed the research. J.C. conducted most of the experiments. R.L. and Y.Z. constructed vectors and injected tobacco. J.M. and J.S. are responsible for checking and revising manuscripts. All authors have read and agreed to the published version of the manuscript.

Funding: The author(s) declare that financial support was received for the research, authorship, and/or publication of this article. This work was funded by the Natural Science Foundation of China (31571956, 32172367), the Natural Science Foundation of Hebei Province (C2020204071), and the Modern Agricultural Industry System of Wheat Industry in Hebei Province (HBCT2023010205).

Data Availability Statement: The data presented in the study are available on request from the corresponding author.

Acknowledgments: We would like to thank Dawei Li of China Agricultural University for being kind in giving us pCaBS-gbLIC and pCaBS-gbPDS (for HIGS-mediated gene silencing), Thank Academician Zhensheng Kang of Northwest A&F University for giving EtHAN.

Conflicts of Interest: The authors declare no conflicts of interest. The funders had no role in the design of the study; in the collection, analyses, or interpretation of data; in the writing of the manuscript; or in the decision to publish the results.

References

1. Tariqjaveed, M.; Mateen, A.; Wang, S.; Qiu, S.; Zheng, X.; Zhang, J.; Bhadauria, V.; Sun, W. Versatile effectors of phytopathogenic fungi target host immunity. *J. Integr. Plant Biol.* **2021**, *63*, 1856–1873. [[CrossRef](#)]
2. Mapuranga, J.; Zhang, N.; Zhang, L.; Chang, J.; Yang, W. Infection strategies and pathogenicity of biotrophic plant fungal pathogens. *Front. Microbiol.* **2022**, *13*, 799396. [[CrossRef](#)]
3. Pradhan, A.; Ghosh, S.; Sahoo, D.; Jha, G. Fungal effectors, the double edge sword of phytopathogens. *Curr. Genet.* **2021**, *67*, 27–40. [[CrossRef](#)]
4. Gabriel, D.W.; Rolfe, B.G. Working models of specific recognition in plant-microbe interactions. *Annu. Rev. Phytopathol.* **1990**, *28*, 365–391. [[CrossRef](#)]
5. Saur, I.M.L.; Hüchelhoven, R. Recognition and defence of plant-infecting fungal pathogens. *J. Plant. Physiol.* **2021**, *256*, 153324. [[CrossRef](#)]
6. Salcedo, A.; Rutter, W.; Wang, S.; Akhunova, A.; Bolus, S.; Chao, S.; Anderson, N.; De Soto, M.F.; Rouse, M.; Szabo, L.; et al. Variation in the *AvrSr35* gene determines *Sr35* resistance against wheat stem rust race Ug99. *Science* **2017**, *358*, 1604–1606. [[CrossRef](#)]
7. Chen, J.; Upadhyaya, N.M.; Ortiz, D.; Sperschneider, J.; Li, F.; Bouton, C.; Breen, S.; Dong, C.; Xu, B.; Zhang, X.; et al. Loss of *AvrSr50* by somatic exchange in stem rust leads to virulence for *Sr50* resistance in wheat. *Science* **2017**, *358*, 1607–1610. [[CrossRef](#)] [[PubMed](#)]
8. Upadhyaya, N.M.; Mago, R.; Panwar, V.; Hewitt, T.; Luo, M.; Chen, J.; Sperschneider, J.; Nguyen-Phuc, H.; Wang, A.; Ortiz, D.; et al. Genomics accelerated isolation of a new stem rust avirulence gene–wheat resistance gene pair. *Nat. Plants* **2021**, *7*, 1220–1228. [[CrossRef](#)] [[PubMed](#)]
9. Dodds, P.N.; Lawrence, G.J.; Catanzariti, A.-M.; Teh, T.; Wang, C.-I.A.; Ayliffe, M.A.; Kobe, B.; Ellis, J.G. Direct protein interaction underlies gene-for-gene specificity and coevolution of the flax resistance genes and flax rust avirulence genes. *Proc. Natl. Acad. Sci. USA* **2006**, *103*, 8888–8893. [[CrossRef](#)]
10. Bryan, G.T.; Wu, K.-S.; Farrall, L.; Jia, Y.; Hershey, H.P.; McAdams, S.A.; Faulk, K.N.; Donaldson, G.K.; Tarchini, R.; Valent, B. A single amino acid difference distinguishes resistant and susceptible alleles of the rice blast resistance gene *Pi-ta*. *Plant Cell* **2000**, *12*, 2033–2045. [[CrossRef](#)]
11. Jia, Y.; McAdams, S.A.; Bryan, G.T.; Hershey, H.P.; Valent, B. Direct interaction of resistance gene and avirulence gene products confers rice blast resistance. *EMBO J.* **2000**, *19*, 4004–4014. [[CrossRef](#)] [[PubMed](#)]

12. Mackey, D.; Holt, B.F.; Wiig, A.; Dangl, J.L. RIN4 interacts with *Pseudomonas syringae* type III effector molecules and is required for RPM1-mediated resistance in Arabidopsis. *Cell* **2002**, *108*, 743–754. [[CrossRef](#)] [[PubMed](#)]
13. van der Hoorn, R.A.; Kamoun, S. From guard to decoy: A new model for perception of plant pathogen effectors. *Plant Cell* **2008**, *20*, 2009–2017. [[CrossRef](#)] [[PubMed](#)]
14. Rafiqi, M.; Bernoux, M.; Ellis, J.G.; Dodds, P.N. In the trenches of plant pathogen recognition: Role of NB-LRR proteins. *Semin. Cell Dev. Biol.* **2009**, *20*, 1017–1024. [[CrossRef](#)]
15. Ade, J.; DeYoung, B.J.; Golstein, C.; Innes, R.W. Indirect activation of a plant nucleotide binding site-leucine-rich repeat protein by a bacterial protease. *Proc. Natl. Acad. Sci. USA* **2007**, *104*, 2531–2536. [[CrossRef](#)]
16. Ma, Z.; Song, T.; Zhu, L.; Ye, W.; Wang, Y.; Shao, Y.; Dong, S.; Zhang, Z.; Dou, D.; Zheng, X.; et al. A *Phytophthora sojae* glycoside hydrolase 12 protein is a major virulence factor during soybean infection and is recognized as a PAMP. *Plant Cell* **2015**, *27*, 2057–2072. [[CrossRef](#)]
17. Ma, Z.; Zhu, L.; Song, T.; Wang, Y.; Zhang, Q.; Xia, Y.; Qiu, M.; Lin, Y.; Li, H.; Kong, L.; et al. A paralogous decoy protects *Phytophthora sojae* apoplastic effector PsXEG1 from a host inhibitor. *Science* **2017**, *355*, 710–714. [[CrossRef](#)]
18. Bozkurt, T.O.; Kamoun, S. The plant-pathogen haustorial interface at a glance. *J. Cell Sci.* **2020**, *133*, jcs237958. [[CrossRef](#)]
19. Mapuranga, J.; Zhang, L.; Zhang, N.; Yang, W. The haustorium: The root of biotrophic fungal pathogens. *Front. Plant Sci.* **2022**, *13*, 963705. [[CrossRef](#)]
20. Segovia, V.; Bruce, M.; Shoup Rupp, J.L.; Huang, L.; Bakkeren, G.; Trick, H.N.; Fellers, J.P. Two small secreted proteins from *Puccinia triticina* induce reduction of β -glucuronidase transient expression in wheat isolines containing Lr9, Lr24 and Lr26. *Can. J. Plant Pathol.* **2016**, *38*, 91–102. [[CrossRef](#)]
21. Zhang, Y.; Wei, J.; Qi, Y.; Li, J.; Amin, R.; Yang, W.; Liu, D. Predicating the effector proteins secreted by *Puccinia triticina* through transcriptomic analysis and multiple prediction approaches. *Front. Microbiol.* **2020**, *11*, 538032. [[CrossRef](#)]
22. Wu, J.Q.; Sakthikumar, S.; Dong, C.; Zhang, P.; Cuomo, C.A.; Park, R.F. Comparative genomics integrated with association analysis identifies candidate effector genes corresponding to *Lr20* in phenotype-paired *Puccinia triticina* isolates from Australia. *Front. Plant Sci.* **2017**, *8*, 148. [[CrossRef](#)]
23. Wu, J.Q.; Dong, C.; Song, L.; Park, R.F. Long-read-based *de novo* genome assembly and comparative genomics of the wheat leaf rust pathogen *Puccinia triticina* identifies candidates for three avirulence genes. *Front. Genet.* **2020**, *11*, 521. [[CrossRef](#)]
24. Cui, Z.; Wu, W.; Fan, F.; Wang, F.; Liu, D.; Di, D.; Wang, H. Transcriptome analysis of *Lr19*-virulent mutants provides clues for the *AvrLr19* of *Puccinia triticina*. *Front. Microbiol.* **2023**, *14*, 1062548. [[CrossRef](#)]
25. Prasad, P.; Jain, N.; Chaudhary, J.; Thakur, R.K.; Savadi, S.; Bhardwaj, S.C.; Gangwar, O.P.; Lata, C.; Adhikari, S.; Kumar, S.; et al. Candidate effectors for leaf rust resistance gene *Lr28* identified through transcriptome and in-silico analysis. *Front. Microbiol.* **2023**, *14*, 1143703. [[CrossRef](#)]
26. Qi, Y.; Li, J.; Mapuranga, J.; Zhang, N.; Chang, J.; Shen, Q.; Zhang, Y.; Wei, J.; Cui, L.; Liu, D.; et al. Wheat leaf rust fungus effector Pt13024 is avirulent to TcLr30. *Front. Plant Sci.* **2022**, *13*, 1098549. [[CrossRef](#)]
27. Wang, F.; Shen, S.; Cui, Z.; Yuan, S.; Qu, P.; Jia, H.; Meng, L.; Hao, X.; Liu, D.; Ma, L.; et al. *Puccinia triticina* effector protein Pt_21 interacts with wheat thaumatin-like protein TaTLP1 to inhibit its antifungal activity and suppress wheat apoplast immunity. *Crop J.* **2023**, *11*, 1431–1440. [[CrossRef](#)]
28. Jones, J.D.G.; Dangl, J.L. The plant immune system. *Nature* **2006**, *444*, 323–329. [[CrossRef](#)]
29. Jones, J.D.G.; Staskawicz, B.J.; Dangl, J.L. The plant immune system: From discovery to deployment. *Cell* **2024**, *187*, 2095–2116. [[CrossRef](#)]
30. Mapuranga, J.; Chang, J.; Zhao, J.; Liang, M.; Li, R.; Wu, Y.; Zhang, N.; Zhang, L.; Yang, W. The underexplored mechanisms of wheat resistance to leaf rust. *Plants* **2023**, *12*, 3996. [[CrossRef](#)]
31. Cloutier, S.; McCallum, B.D.; Loutre, C.; Banks, T.W.; Wicker, T.; Feuillet, C.; Keller, B.; Jordan, M.C. Leaf rust resistance gene *Lr1*, isolated from bread wheat (*Triticum aestivum* L.) is a member of the large *psr567* gene family. *Plant Mol. Biol.* **2007**, *65*, 93–106. [[CrossRef](#)] [[PubMed](#)]
32. Shao, D.; Smith, D.L.; Kabbage, M.; Roth, M.G. Effectors of plant necrotrophic fungi. *Front. Plant Sci.* **2021**, *12*, 687713. [[CrossRef](#)]
33. Zhao, S.; Shang, X.; Bi, W.; Yu, X.; Liu, D.; Kang, Z.; Wang, X.; Wang, X. Genome-wide identification of effector candidates with conserved motifs from the wheat leaf rust fungus *Puccinia triticina*. *Front. Microbiol.* **2020**, *11*, 1188. [[CrossRef](#)]
34. Cui, Z.; Shen, S.; Meng, L.; Sun, X.; Jin, Y.; Liu, Y.; Liu, D.; Ma, L.; Wang, H. Evasion of wheat resistance gene recognition by the leaf rust fungus is attributed to the coincidence of natural mutations and deletion in gene. *Mol. Plant Pathol.* **2024**, *25*, e13490. [[CrossRef](#)]
35. Catanzariti, A.-M.; Dodds, P.N.; Lawrence, G.J.; Ayliffe, M.A.; Ellis, J.G. Haustorially expressed secreted proteins from flax rust are highly enriched for avirulence elicitors. *Plant Cell* **2006**, *18*, 243–256. [[CrossRef](#)]
36. Bourras, S.; Kunz, L.; Xue, M.; Praz, C.R.; Müller, M.C.; Kälin, C.; Schläfli, M.; Ackermann, P.; Flückiger, S.; Parlange, F.; et al. The AvrPm3-Pm3 effector-NLR interactions control both race-specific resistance and host-specificity of cereal mildews on wheat. *Nat. Commun.* **2019**, *10*, 2292. [[CrossRef](#)] [[PubMed](#)]
37. McNally, K.E.; Menardo, F.; Lüthi, L.; Praz, C.R.; Müller, M.C.; Kunz, L.; Ben-David, R.; Chandrasekhar, K.; Dinoor, A.; Cowger, C.; et al. Distinct domains of the AVRPM3(A2/F2) avirulence protein from wheat powdery mildew are involved in immune receptor recognition and putative effector function. *New Phytol.* **2018**, *218*, 681–695. [[CrossRef](#)]

38. Jumper, J.; Evans, R.; Pritzel, A.; Green, T.; Figurnov, M.; Ronneberger, O.; Tunyasuvunakool, K.; Bates, R.; Žídek, A.; Potapenko, A.; et al. Highly accurate protein structure prediction with AlphaFold. *Nature* **2021**, *596*, 583–589. [[CrossRef](#)] [[PubMed](#)]
39. Varadi, M.; Anyango, S.; Deshpande, M.; Nair, S.; Natassia, C.; Yordanova, G.; Yuan, D.; Stroe, O.; Wood, G.; Laydon, A.; et al. AlphaFold protein structure database: Massively expanding the structural coverage of protein-sequence space with high-accuracy models. *Nucleic Acids Res.* **2022**, *50*, D439–D444. [[CrossRef](#)]
40. Kamoun, S. A catalogue of the effector secretome of plant pathogenic oomycetes. *Annu. Rev. Phytopathol.* **2006**, *44*, 41–60. [[CrossRef](#)]
41. Long, D.L.; Kolmer, J.A. A North American system of nomenclature for *Puccinia recondita* f. sp. tritici. *Phytopathology* **1989**, *79*, 525–529. [[CrossRef](#)]
42. Yin, W.; Wang, Y.; Chen, T.; Lin, Y.; Luo, C. Functional evaluation of the signal peptides of secreted proteins. *Bio. Protoc.* **2018**, *8*, e2839. [[CrossRef](#)] [[PubMed](#)]
43. Yang, Q.; Huai, B.; Lu, Y.; Cai, K.; Guo, J.; Zhu, X.; Kang, Z.; Guo, J. A stripe rust effector Pst18363 targets and stabilises TaNUDX23 that promotes stripe rust disease. *New Phytol.* **2020**, *225*, 880–895. [[CrossRef](#)] [[PubMed](#)]
44. Wei, J.; Wang, X.; Hu, Z.; Wang, X.; Wang, J.; Wang, J.; Huang, X.; Kang, Z.; Tang, C. The *Puccinia striiformis* effector Hasp98 facilitates pathogenicity by blocking the kinase activity of wheat TaMAPK4. *J. Integr. Plant Biol.* **2023**, *65*, 249–264. [[CrossRef](#)] [[PubMed](#)]
45. Qi, T.; Guo, J.; Liu, P.; He, F.; Wan, C.; Islam, M.A.; Tyler, B.M.; Kang, Z.; Guo, J. Stripe rust effector PstGSRE1 disrupts nuclear localization of ROS-promoting transcription factor TaLOL2 to defeat ROS-induced defense in wheat. *Mol. Plant* **2019**, *12*, 1624–1638. [[CrossRef](#)]
46. Duan, Z.; Xu, H.; Ji, X.; Zhao, J.; Xu, H.; Hu, Y.; Deng, S.; Hu, S.; Liu, X. Importin $\alpha 5$ negatively regulates importin $\beta 1$ -mediated nuclear import of Newcastle disease virus matrix protein and viral replication and pathogenicity in chicken fibroblasts. *Virulence* **2018**, *9*, 783–803. [[CrossRef](#)] [[PubMed](#)]
47. Yuan, C.; Li, C.; Yan, L.; Jackson, A.O.; Liu, Z.; Han, C.; Yu, J.; Li, D. A high throughput barley stripe mosaic virus vector for virus induced gene silencing in monocots and dicots. *PLoS ONE* **2011**, *6*, e26468. [[CrossRef](#)] [[PubMed](#)]

Disclaimer/Publisher’s Note: The statements, opinions and data contained in all publications are solely those of the individual author(s) and contributor(s) and not of MDPI and/or the editor(s). MDPI and/or the editor(s) disclaim responsibility for any injury to people or property resulting from any ideas, methods, instructions or products referred to in the content.